

Superconductivity and magnetism in the pseudoternary system $\text{Gd}_x\text{Y}_{1-x}\text{Rh}_4\text{B}_4$

H. Adrian, R. Müller, and R. Behrle

*Physikalisches Institut der Universität Erlangen-Nürnberg,**D-8520 Erlangen, Bundesrepublik Deutschland*

(Received 22 February 1982)

The phase boundaries between the paramagnetic, superconducting, and ferromagnetically ordered states of the tetragonal pseudoternary system $\text{Gd}_x\text{Y}_{1-x}\text{Rh}_4\text{B}_4$ have been determined by ac susceptibility measurements. Magnetization measurements, performed with cylindrical samples for $0 \leq x \leq 0.45$ at temperatures above 1.5 K, show clearly that macroscopic electromagnetic effects are of minor importance in this system and indicate a transition from type-II/2 to type-II/1 or type-I superconductivity at temperatures close to T_{c2} . For the critical fields we obtain from the magnetization curves a sawtoothlike $H_{c1}(T)$, scaling with $T_{c1}(x)$, whereas $H_{c2}(T)$ is bell shaped for $x \geq 0.1$, with its maximum decreasing exponentially with x for $x \leq 0.30$. From Arrott plots we find spontaneous magnetizations below T_m and Curie-Weiss laws for the normal-state susceptibility indicating ferromagnetic Curie temperatures $\Theta_c > 0$ for $x > 0.1$. Analyzing the data we show that the strength of the exchange interaction between the conduction electrons and the Gd moments deduced from $T_{c1}(x)$ is strong enough to mediate the indirect interaction between the Gd moments as found from $\Theta_c(x)$. From specific-heat measurements carried out for $x=0.25$ and 0.45 we obtain $N^*(E_F)=0.57$ states/(atom eV spin), in agreement with the nonmagnetic Y and Lu compounds. The details of the magnetic transitions appear to scale with the Gd concentration.

I. INTRODUCTION

The discovery of either superconductivity or magnetic order in the CeCo_4B_4 -type rare-earth (R) rhodium boride compound series RRh_4B_4 , reported by Matthias and co-workers,^{1,2} followed by the discovery of reentrant superconductivity in ErRh_4B_4 ,³ has motivated many physicists to study in detail the interplay between superconductivity and magnetism.⁴ Since then, many ternary and pseudoternary compounds have been reported to exhibit superconductivity as well as magnetic order of rare-earth ions. In the case of antiferromagnetism, superconductivity has been found to coexist, whereas no coexistence with uniform ferromagnetic order has been observed so far. However, recent neutron scattering experiments on a ErRh_4B_4 single crystal indicate the existence of a small temperature range ($0.7 < T < 1.2$ K for the particular sample investigated) where a transverse, linearly polarized, sinusoidally modulated ferromagnetic state (wavelength ~ 100 Å) coexists with superconductivity. This intermediate state is strongly suppressed by very weak magnetic fields.⁵

The phase transition from superconductivity to ferromagnetic order is connected with anomalies observed in many physical properties, such as elec-

trical resistivity,³ specific heat,⁶ or low-temperature magnetization.⁷⁻⁹ The existence of a series of isostructural compounds offers the possibility of studying pseudoternary systems,¹⁰⁻²⁵ which allows one to gradually change the relative strength of the interactions concerned.

Although no zero-field properties can be observed, low-temperature magnetization measurements are able to provide interesting information on the microscopic mechanism responsible for the phase transition. In an earlier paper⁸ on the $\text{Er}_{1-x}\text{Ho}_x\text{Rh}_4\text{B}_4$ system we reported the first experimental evidence for a transition from type-II/2 to type-II/1 or type-I superconductivity at temperatures close to T_{c2} , which denotes the transition temperature from superconductivity to the normal state upon cooling. This particular feature was predicted earlier by Tachiki *et al.*^{26,27} The $\text{Er}_{1-x}\text{Ho}_x\text{Rh}_4\text{B}_4$ system is of special interest, because the Er compound becomes superconducting at $T_{c1} \approx 8.7$ K and normal and ferromagnetic at $T_{c2} \approx 0.9$ K, whereas the Ho compound is ferromagnetic below 7 K.¹⁰ However, a complication arises because both end compounds contain magnetic ions, which furthermore align along different directions in the ferromagnetic state.²⁸ An additional problem could enter through crystalline electric-field effects which

seem to be of significance in these compounds.¹⁸ We therefore continued our study with measurements of the isostructural $\text{Gd}_x\text{Y}_{1-x}\text{Rh}_4\text{B}_4$ system, which contains only one kind of magnetic ion, Gd^{3+} , which moreover is a pure S state; crystalline-field effects should therefore be negligible. In this paper we report the phase diagram of the $\text{Gd}_x\text{Y}_{1-x}\text{Rh}_4\text{B}_4$ system, low-temperature magnetization measurements for Gd concentrations $0 \leq x \leq 0.45$ and specific-heat measurements for $x=0.25$ and 0.45 .

II. EXPERIMENTAL

Samples of 1-g mass were prepared for nominal compositions $0 \leq x \leq 0.45$ by arc-melting the appropriate amounts of the high-purity elements in a zircon-gettered argon atmosphere. In order to enhance the homogeneity, the samples were turned over and remelted several times, sealed in tantalum tubes, and annealed at 1050°C for 14 d. After the heat treatment, the temperature was slowly reduced ($30^\circ\text{C}/30$ min) to avoid cracks. For dc-magnetization measurements, cylinders of about 6-mm length and 1-mm diameter were spark-cut out of the nearly spherical ingots. The demagnetization factor of the cylinders is estimated to be 0.05. The tetragonal phase with $a=5.31$ Å and $c=7.41$ Å was established by x-ray diffraction experiments with pulverized parts of the original samples and with $\text{Cu } K\alpha_1$ radiation in Seemann-Bohlin geometry with a monochromator. The x-ray data additionally showed that a very small amount of an unidentified impurity phase is present in the samples. The cylinders were sealed in tantalum tubes for a second time and annealed at 1050°C for another three days to reduce lattice defects at the surface which might have been produced during the spark cutting.

The phase diagram was determined from the spherical ingots by a standard ac mutual-inductance bridge for temperatures $T \geq 1.2$ K. Magnetization measurements of the cylinders were carried out using concentric pick-up coils and a linear sweep of the external magnetic field. The induced dc voltage, giving the differential susceptibility, was fed into a PDP-11 computer via CAMAC. Simultaneously the magnetization was obtained by analog integration. The specific heat of the cylinders with $x=0.25$ and 0.45 , each having a mass of about 40 mg, was measured with an adiabatic heat-pulse method using a microcalorimeter. The lowest obtainable temperatures were 1.5 K for the magnetization experiments and 1.9 K for the specific-heat measurements.

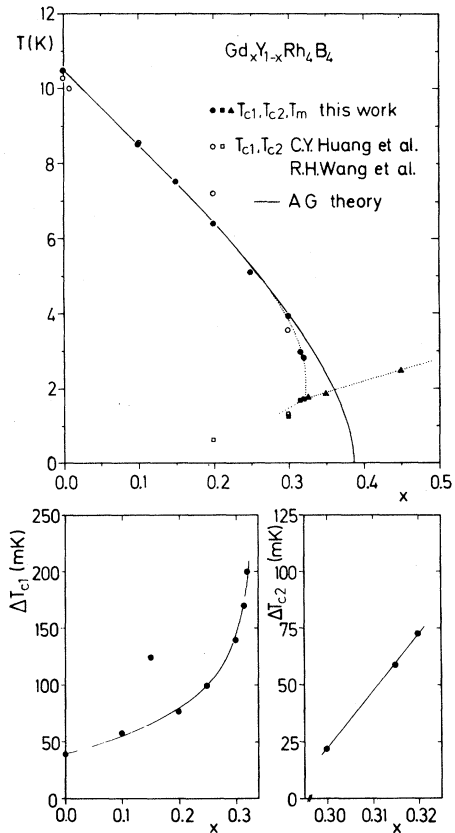


FIG. 1. Phase diagram for $\text{Gd}_x\text{Y}_{1-x}\text{Rh}_4\text{B}_4$ between the paramagnetic, superconducting and ferromagnetically ordered state (upper part) measured by ac susceptibility. The respective transition widths at T_{c1} and T_{c2} are shown in the lower part.

III. RESULTS AND DISCUSSION

A. Phase diagram

The phase diagram between the paramagnetic, superconducting, and ferromagnetically ordered states is shown in the upper part of Fig. 1. T_{c1} was determined as the midpoint of the transition from the normal, paramagnetic state to the superconducting state and T_{c2} as the midpoint of the transition from the superconducting state to the peak in the ac susceptibility which accompanies the normal magnetically ordered state. The transition widths ΔT_{c1} and ΔT_{c2} , shown in the lower part of Fig. 1, are defined as the temperature differences between 10% and 90% of the respective signal change.

For Gd concentrations up to $x=0.30$, T_{c1} follows Abrikosov-Gorkov (AG) theory²⁹ with a critical concentration $x_{cr}=0.385$, indicating a weak exchange interaction between the spins of the conduction electrons responsible for superconductivity (Rh

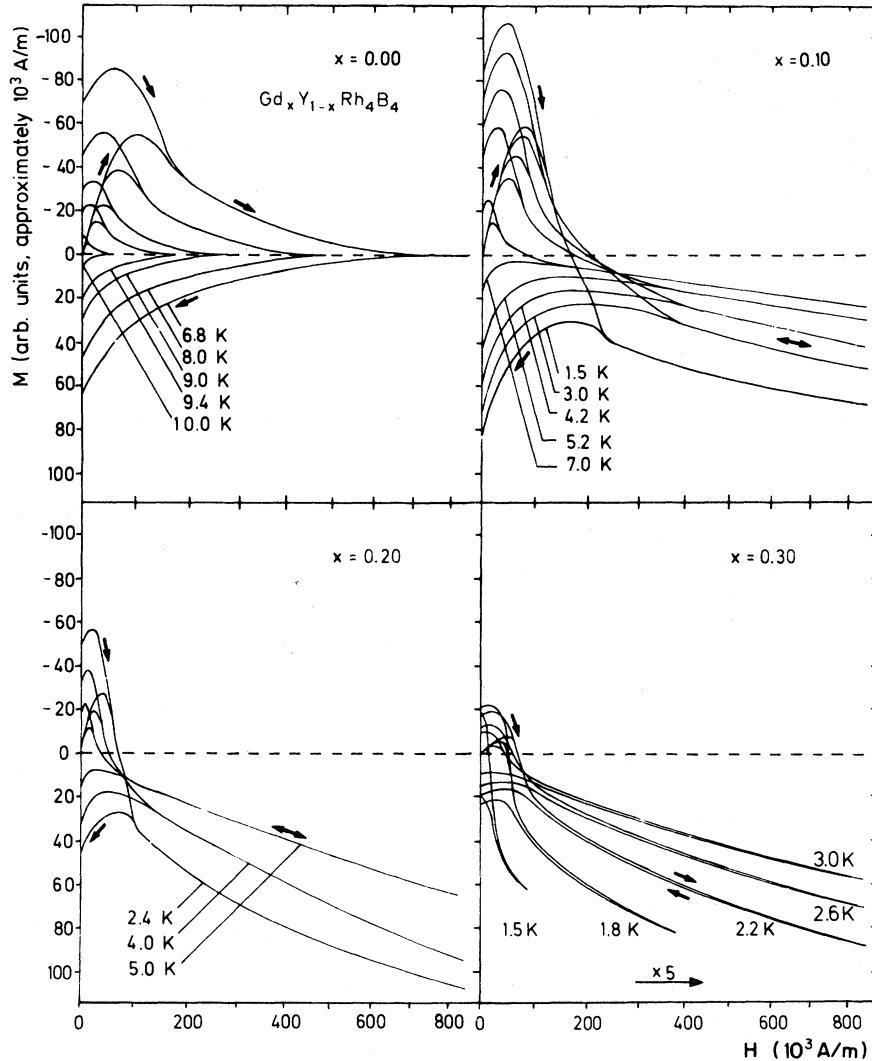


FIG. 2. Selection of typical magnetization curves for different Gd concentrations and various temperatures. The curves beginning at $M=0$ are the virgin curves. Only one field direction of the full hysteresis curves taken is shown. The sequence of the different branches can be obtained by a comparison with Fig. 4. Note that for $x=0.30$ the curves are expanded along the H axis by a factor of 5.

d electrons) and the Gd magnetic moment. This is conceivable considering the cluster character of the Rh tetrahedra and is also in agreement with self-consistent linear muffin-tin orbital energy band calculations.³⁰ According to AG theory, the initial slope of the $T_{c1}(x)$ depression $(dT_{c1}/dx)_{x=0}$ is given by

$$9 \left(\frac{dT_{c1}}{dx} \right)_{x=0} = - \frac{\pi^2 N(E_F)}{2k_B} \mathcal{J}^2 (g_J - 1)^2 \times J(J+1). \quad (1)$$

Using $N(E_F)=0.35$ states/(eV atom spin), $g_J=2$,

$J=\frac{7}{2}$ for Gd^{3+} , and from Fig. 1 $(dT_{c1}/dx)_{x=0} = -20$ K per atom fraction, we obtain for the magnitude of the exchange coupling constant $|\mathcal{J}|=24$ meV which is in agreement with the $Lu_{1-x}Gd_xRh_4B_4$ system studied by MacKay *et al.*²⁵ For $x > 0.30$, reentrant behavior with $T_{c2} > 1.2$ K is observed. For x in the vicinity of 0.325, T_{c1} decreases very fast; whereas the sample with the nominal composition $x=0.320$ is superconducting in the interval $1.72 \leq T \leq 2.82$ K, for $x=0.325$ only a transition to a magnetically ordered state is found at $T_m=1.77$ K. This strong concentration dependence is also reflected in the transition widths, shown in the lower part of Fig. 1. Howev-

er, even for $x=0.32$, the transition widths are small compared to the superconducting region and a full diamagnetic ac-susceptibility signal was measured. For $x \geq 0.325$, the magnetic ordering temperature T_m increases linearly with x and extrapolates for $x=1$ to $T_m=5.6$ K, which is in agreement with what is found for GdRh_4B_4 . Figure 1 also shows T_{c1} and T_{c2} data reported by Wang *et al.*¹² and Huang *et al.*¹³ which in general correspond well to our results.

B. Magnetization curves

A representative selection of magnetization curves for four different Gd concentrations is shown in Fig. 2. The magnetization curves are not corrected for demagnetization effects, which are relatively small in this system (see below). However, this correction has been applied for other data given in this paper, e.g., critical fields and susceptibility. For samples with $x=0.0, 0.15, 0.20, 0.25, 0.30, 0.315,$ and 0.32 , data similar as shown in Fig. 2 were taken within the superconducting temperature region in intervals of about 0.2 K. In extension of Fig. 2, complete hysteresis curves were measured in all cases. The general shape of the magnetization curves of $\text{Gd}_x\text{Y}_{1-x}\text{Rh}_4\text{B}_4$ is similar to those of the $\text{Er}_{1-x}\text{Ho}_x\text{Rh}_4\text{B}_4$ system reported earlier, exhibiting a purely diamagnetic Meissner state, a mixed state that clearly consists of a superconducting and a

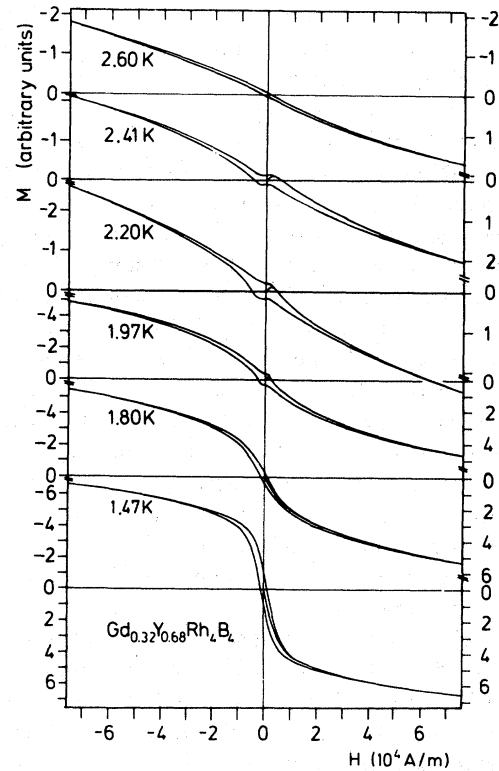


FIG. 3. Full hysteresis curves for $x=0.32$. The temperatures vary from about T_{c1} to below T_{c2} . Note that the M axis of the three upper curves is expanded by a factor of 2.5 compared to the three lower curves.

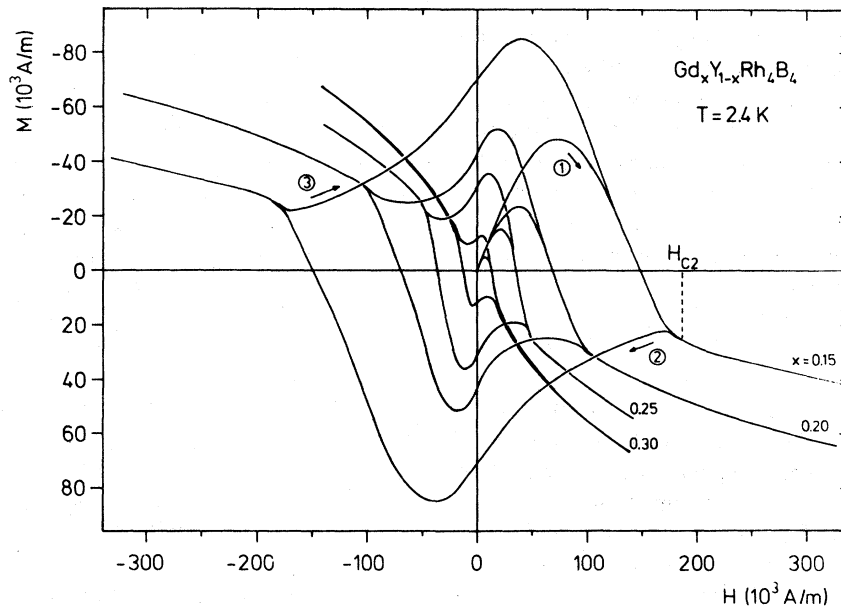


FIG. 4. Full hysteresis curves of $\text{Gd}_x\text{Y}_{1-x}\text{Rh}_4\text{B}_4$ for various Gd concentrations taken at 2.4 K. The arrows and encircled numbers indicate direction and sequence of the different branches beginning with virgin curves at $M=0$.

paramagnetic contribution due to the Gd ions for $x > 0$, and a normal paramagnetic state. It is evident that with increasing Gd concentration and decreasing temperature the paramagnetic behavior becomes more pronounced. Further, extremely irreversible characteristics are revealed which are not correlated with the fraction of magnetic ions and seem generally to occur in the ternary borides.³¹ The transition from the Meissner state to the mixed state cannot be clearly detected, presumably due to retarded flux entry caused by pinning effects. Therefore, we defined H_{c1} as the field where $M(H)$ first deviates from the straight line. For $x \leq 0.20$, the field where the hysteretic behavior starts is unambiguously identifiable when the magnetic field is reduced from high values. Contrary to this, for higher Gd concentrations, a very small hysteresis occurs even in the field region where superconductivity is expected to be quenched by comparison with the low- x data. This is shown in Fig. 2 for $x = 0.30$, but has been observed for all samples with $x \geq 0.25$. Similar results have been reported for ErRh_4B_4 earlier.^{9,32} Consequently we believe H_{c2} is approximately given by the field where the large hysteresis loop opens. Usually slightly above this point a small kink in the $M(H)$ curves is present, and the corresponding field was taken as H_{c2} . The width of the small hysteresis observed in the normal state in fields exceeding H_{c2} appears to increase slightly with x and with decreasing temperature and to develop continuously into the behavior found at temperatures below T_{c2} . This is displayed in Fig. 3 for $x = 0.32$.

At temperatures approaching T_{c2} , the part of the magnetization curves between H_{c1} and H_{c2} becomes steeper and H_{c2} rapidly decreases, while H_{c1} still increases. This indicates a transition from type-II/2 to type-II/1 or type-I superconductivity as reported for the $\text{Er}_{1-x}\text{Ho}_x\text{Rh}_4\text{B}_4$ system and theoretically predicted.²⁶ The correction for demagnetizing effects still increases the slope of the positive part of the magnetization curves.

Although it was not possible to observe details of this transition experimentally, since H_{c1} is poorly defined and no kink is present in the curves, it is evident that the normal-state susceptibility is of great importance. This can also be seen in Fig. 4 which shows complete magnetization curves taken at 2.4 K for various Gd concentrations. The critical fields H_{c1} and H_{c2} as defined above could usually be more unambiguously identified in the differential susceptibility dM/dH , which was simultaneously recorded. A typical example is displayed in Fig. 5.

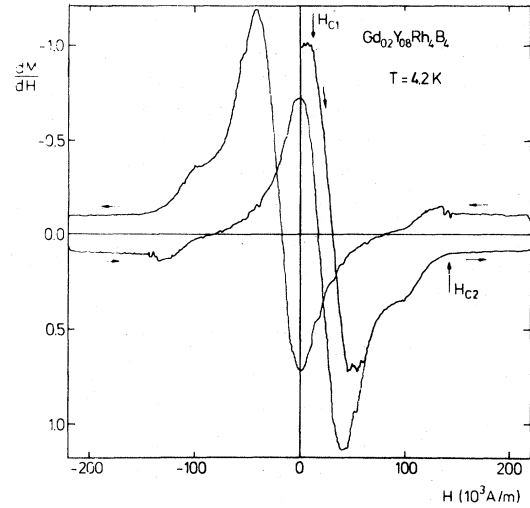


FIG. 5. Example for the voltage induced in the balanced pick-up coils which corresponds to the differential susceptibility dM/dH . The poorly defined H_{c1} can be more easily determined.

C. Critical magnetic fields

Within the experimental error, the temperature dependence of the lower critical field $H_{c1}(T)$, plotted in Fig. 6, scales with T_{c1} with an approximately constant initial slope $(dH_{c1}/dT)_{T=T_{c1}}$, as was found for the $\text{Er}_{1-x}\text{Ho}_x\text{Rh}_4\text{B}_4$ system. For comparable

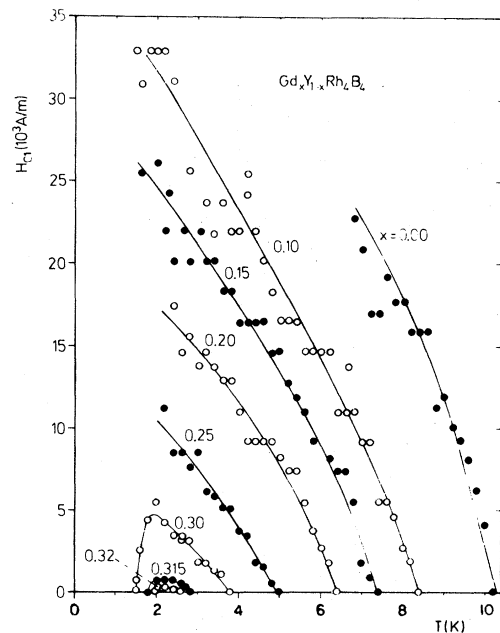


FIG. 6. Temperature dependence of the lower critical field $H_{c1}(T)$ for various Gd concentrations. The lines are drawn as a guide to the eye.

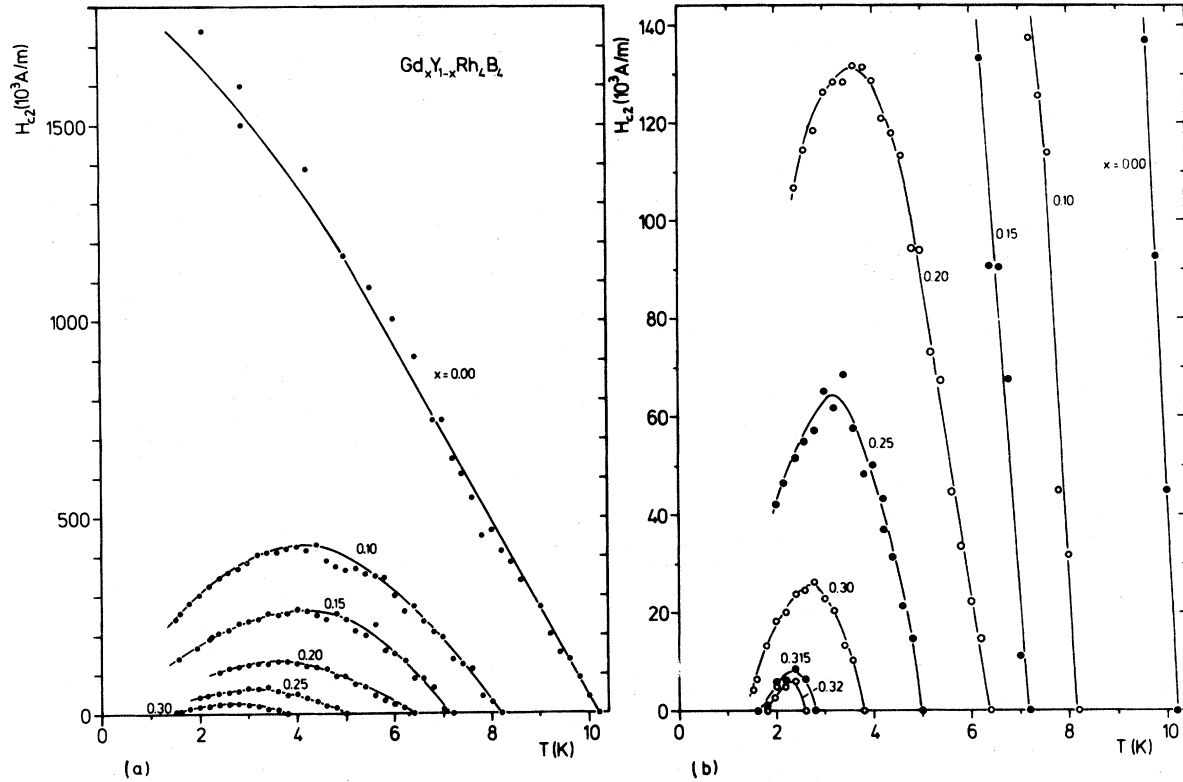


FIG. 7. Temperature dependence of the upper critical field $H_{c2}(T)$ for various Gd concentrations. Note the extremely expanded H_{c2} axis in (b).

T_{c1} between 7 and 9 K, $H_{c1}(T)$ is about 50% larger in the $Gd_xY_{1-x}Rh_4B_4$ system than in the $Er_{1-x}Ho_xRh_4B_4$ system (e.g., 3×10^4 A/m compared to 2×10^4 A/m). Qualitatively similar in both systems is the steep decrease of H_{c1} in a small temperature interval (~ 0.2 K) above T_{c2} . The scaling behavior of H_{c1} indicates that the pair-breaking mechanism described by AG theory, which is responsible for the T_{c1} depression with increasing x , is sufficient to account for the decrease of $H_{c1}(T)$ and is not strongly temperature dependent.

Quite different is the temperature dependence of the upper critical field $H_{c2}(T)$, shown in Fig. 7. For all samples with $x \geq 0.10$, $H_{c2}(T)$ is smoothly bell shaped with no indication of a low-temperature anomaly as reported for the $Er_{1-x}Ho_xRh_4B_4$ system. There are more noteworthy differences: The initial slope $(dH_{c2}/dT)_{T=T_{c1}}$ and the maximum of H_{c2} decrease rapidly with increasing x . $H_{c2}(T)$ does not scale with T_{c1} . The positive magnetization of the Gd ions at H_{c2} , hereafter denoted M_{c2} , is small compared to H_{c2} , except for very low temperatures. This means macroscopic electromagnetic interactions are only of minor significance. Therefore, the failure of $H_{c2}(T)$ to scale with T_{c1} is not

due to M_{c2} , since

$$B_{c2}^*(T) = \frac{B_{c2}(T)}{\mu_0} = H_{c2}(T) + M_{c2}(T)$$

is similar to $H_{c2}(T)$.

Up to $x=0.30$, the dependence of the maximum of the $H_{c2}(T)$ curves, $H_{c2,max}$, on x is well described by

$$H_{c2,max}(x) = H_{c2}(x=0, T=0) \exp(-ax), \quad (2)$$

with $a=13.8$ and the extrapolated critical field $H_{c2}(x=0, T=0) = 2 \times 10^6$ A/m (this corresponds to 25 kOe). From this follows the linear x dependence of $\log(H_{c2,max})$ vs x plotted in Fig. 8(a). The data of Fig. 7 exhibit another interesting feature involving the temperature $T_{max}(x)$ where the maximum of $H_{c2}(T)$ occurs, shown in Fig. 8(b): For low x there must be an increase of $T_{max}(x)$ from zero. However, since we did not measure samples with $0 < x < 0.1$, this increase could be different from the one indicated by the dashed line in Fig. 8(b). For higher Gd concentrations $T_{max}(x)$ does not monotonically increase, but decreases with x . The same is true if one considers the $B_{c2}^*(T)$ data instead.

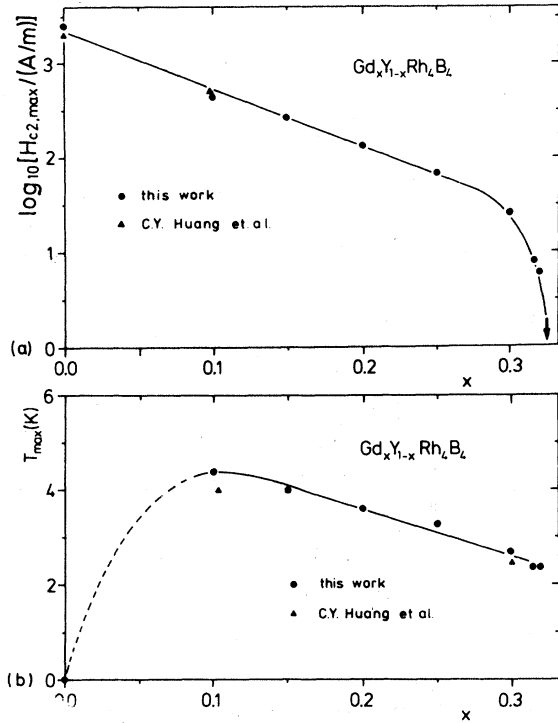


FIG. 8. (a) Logarithmic plot of the maximum of $H_{c2}(T)$ vs Gd concentration x . (b) Temperature $T_{max}(x)$ where the maximum in $H_{c2}(T)$ occurs vs Gd concentration x .

D. Normal-state susceptibility and magnetic order

From the magnetization data we calculated the normal-state susceptibility

$$\chi(T) = M_{c2}(T)/H_{c2}(T).$$

Figure 9, where χ^{-1} is plotted versus temperature, shows that the data are consistent with Curie-Weiss laws considering the experimental scatter present. From an extrapolation of the straight lines to $\chi^{-1}=0$, we obtain tentative Curie temperatures which point toward ferromagnetic behavior for $x > 0.10$. In order to investigate in more detail the occurrence of a spontaneous magnetization we calculated Arrott plots (M^2 vs H/M) from the continuously measured magnetization curves. Three examples are shown in Fig. 10. In small to moderate fields ($H < 10^5$ A/m), M^2 should be linear with H/M . The extrapolation to $M^2=0$ intercepts the H/M axis at the "zero-field" inverse susceptibility. A negative intercept corresponds to spontaneous magnetization. The slope S of the straight lines M^2 vs H/M is theoretically expected to vary as

$$S(x, T) \propto \frac{1}{T} x^3. \quad (3)$$

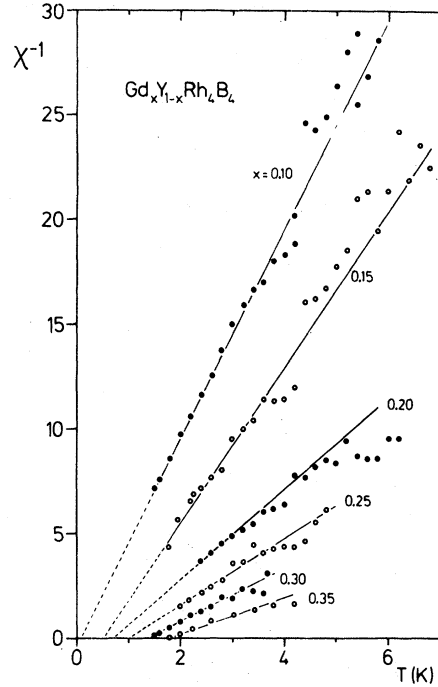


FIG. 9. Inverse normal-state susceptibility χ^{-1} vs temperature as obtained at H_{c2} .

From this it follows that ST/x^3 should be constant. In our experiment this was true within a factor of 2, although for $1.5 \leq T \leq 10$ K and $0.10 \leq x \leq 0.35$ the slope S itself varies about a factor of 300. The susceptibility data taken from the Arrott plots, again, give Curie-Weiss laws similar to those shown in Fig. 9, except for the Curie temperatures which tend to be about 0.2 K higher. For comparison, Fig. 11(a) shows the magnetic ordering temperatures as obtained from the Arrott plot, the M_{c2}/H_{c2} data, and ac susceptibility. Within the experimental error we cannot observe a definite difference. It should be noted that for $x \leq 0.30$ the Curie temperatures are obtained by extrapolation of the susceptibility data.

Oguchi and Obokata³³ calculated the dependence of the Curie temperature on the Gd concentration using an effective Hamiltonian method based on the Ising model and the Heisenberg model to account for magnetic moments diluted by nonmagnetic atoms. For a ferromagnet they obtain

$$\frac{I}{k_B \Theta_c} = \frac{1}{21} \frac{1}{1+n} \ln \left[\frac{x'(z-1)+1}{x'(z-1)-1-2n} \right], \quad (4)$$

where I is the interaction parameter for two magnetic moments on nearest-neighbor sites, z is the

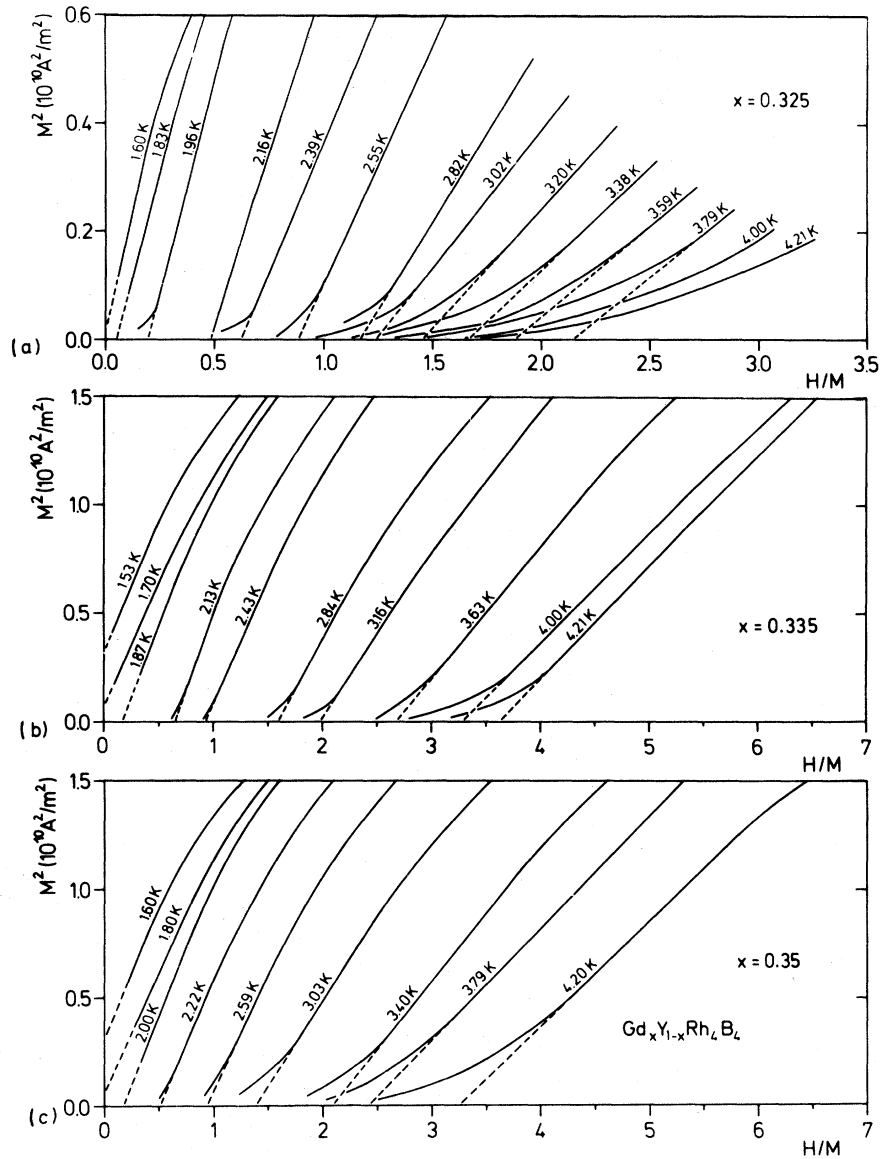


FIG. 10. Selection of Arrott plots M^2 vs H/M for three different Gd concentrations at various temperatures. The plots were calculated from the continuously measured $M(H)$ curves.

number of nearest neighbors, considering here only R atoms, $n=0$ for Ising model and $n=1$ for Heisenberg model, and x' is the concentration of nonisolated magnetic moments obtained from x by

$$x' = x[1 - (1-x)^z]. \quad (5)$$

The factor 21 accounts for the total angular momentum $J = \frac{7}{2}$ and is given by

$$J(J+1)/[\frac{1}{2}(\frac{1}{2}+1)].$$

The result of this theory is shown in Fig. 11(b). The data are consistent with the Ising model ($z=12$)

with $I=3.8 \mu\text{eV}$. The coordination $z=12$ agrees with the R sublattice which can be considered as slightly distorted face-centered cubic. The failure of the Heisenberg model to fit the data shows that the direct exchange interaction is not important, as expected from the large R - R distances.

The value of \mathcal{J} obtained from the depression of T_{c1} is large enough to account for the ion-ion interaction I deduced from the Curie temperatures, since $\mathcal{J}^2 > I/N(E_F)$. From this we conclude that the exchange interaction between the conduction electrons and the R magnetic moments is strong

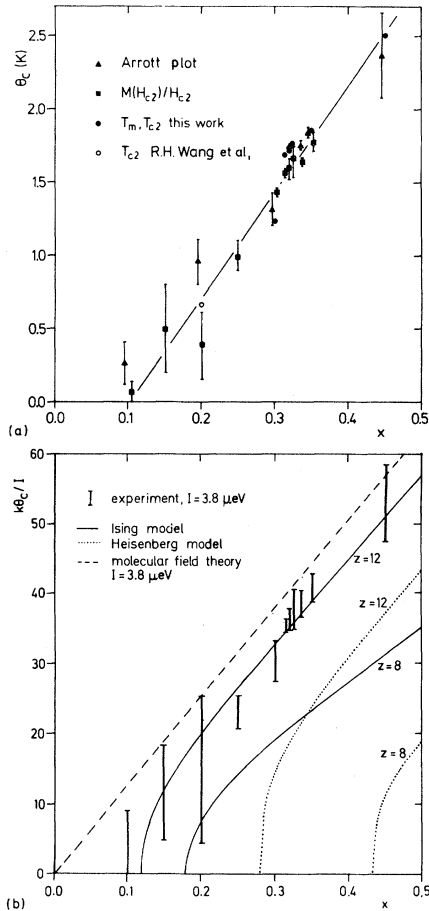


FIG. 11. (a) Magnetic ordering temperatures Θ_c of $\text{Gd}_x\text{Y}_{1-x}\text{Rh}_4\text{B}_4$, obtained by different methods as described in the text, vs Gd concentration. (b) Comparison of the measured ordering temperatures with the theoretical result of Oguchi and Obokata (Ref. 33) for diluted ferromagnets. Agreement is obtained for the Ising model with $z=12$ using $I=3.8 \mu\text{eV}$.

enough to be responsible for the indirect exchange interaction between the R ions.

E. High-field magnetization

For several Gd concentrations high-field magnetization measurements were carried out in fields up to $8 \times 10^5 \text{ A/m}$ ($\sim 10 \text{ kOe}$) or $5 \times 10^6 \text{ A/m}$ ($\sim 65 \text{ kOe}$). Three examples are shown in Figs. 12 and 13. On the average we observe a magnetic moment which is only about 70–80% of the free-ion value. Furthermore it appears that at low temperatures, where the Arrott plots reveal spontaneous magnetizations, the high-field curves cross those taken at slightly higher temperatures. These effects could

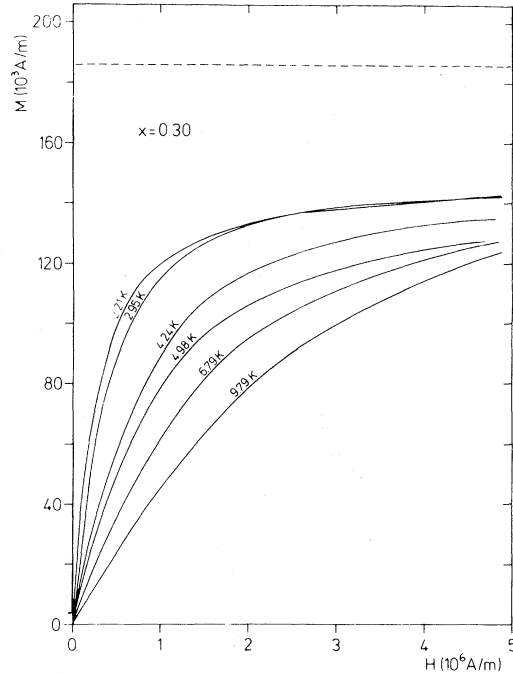


FIG. 12. High-field magnetization for $x=0.30$ at various temperatures. The dashed line corresponds to the magnetic moments of free Gd^{3+} ions ($5 \times 10^6 \text{ A/m}$ is equivalent to 62.83 kOe).

indicate the existence of anisotropy effects other than crystalline fields which should be of no importance in the case of Gd^{3+} ions. This is also supported by the linear x dependence of the ordering temperature in the $\text{Er}_{1-x}\text{Gd}_x\text{Rh}_4\text{B}_4$ system,¹² from which one might conclude that the Gd moment is oriented within the tetragonal basal plane, as found for ErRh_4B_4 by neutron scattering. If we speculate that a strong anisotropy exists which aligns the Gd moment along two perpendicular equivalent lines (four directions) and the effect of the external field being reduced to change the moments to the direction with the largest component parallel to the field, we calculate for a polycrystalline sample a macroscopic moment which is 71% of the local moment. Although this argument is not conclusive, there is some more experimental evidence. Anisotropy effects could also explain the occurrence of hysteretic behavior in the magnetization curves above T_{c2} if they maintain some strength at temperatures where uniform long-range order still does not exist.

F. Specific heat

For $x=0.25$ and 0.45 the specific heat was measured at temperatures between 2 and 20 K. The re-

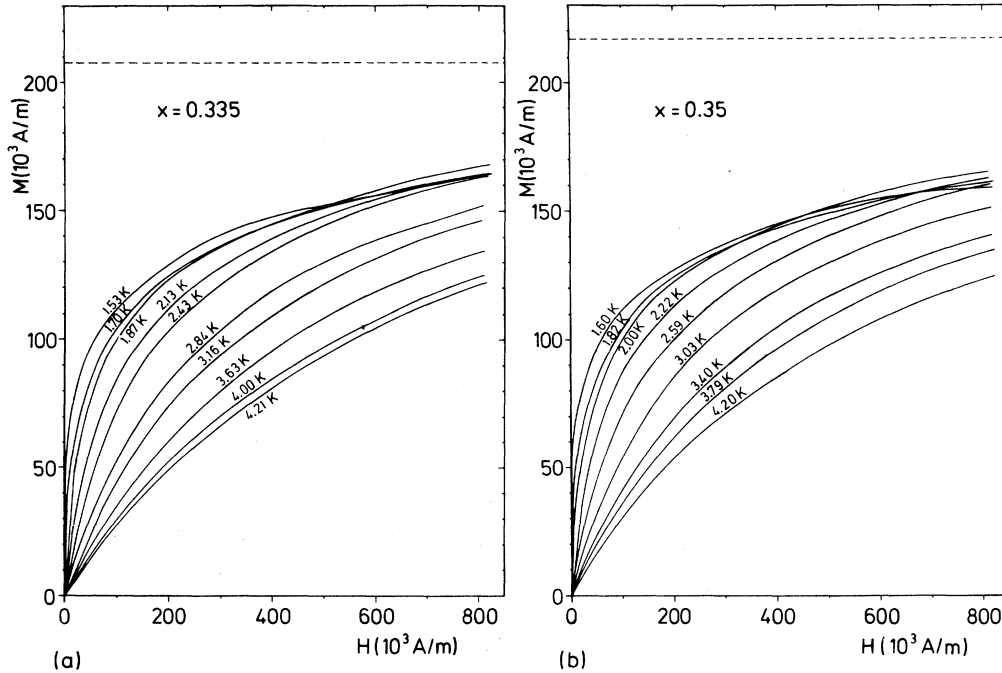


FIG. 13. High-field magnetization for (a) $x=0.335$ and (b) $x=0.35$ at various temperatures. Note that the curves taken at $T < T_m$ intersect those taken at $T > T_m$. The dashed lines correspond to the magnetic moments of free Gd^{3+} ions.

sults are shown in Fig. 14. In the case of $x=0.25$, the data taken in the interval $8 \leq T \leq 16$ K could be well fitted with a linear and a cubic term, giving a coefficient of the electronic specific heat $\gamma=24$ mJ/molK² and a Debye temperature $\Theta_D=174$ K. The data of the $x=0.45$ sample are consistent with the same γ and $\Theta_D=163$ K, which correlates well with the change of the average mass of the third element (TE),

$$\Theta_D(x=0.45) = \left[\frac{\langle M_{\text{TE},0.25} \rangle}{\langle M_{\text{TE},0.45} \rangle} \right]^{1/2} \Theta_D(x=0.25)$$

indicating that the corresponding modes are the dominant contribution to the lattice specific heat at low temperature. From γ we calculate a renormalized electronic density of states $N^*(E_F)=0.57$ states/(eV atom spin) in good agreement with other experiments.^{34,35} Using for the bare density of states $N(E_F)=0.35$ states/(eV atom spin) obtained from band-structure calculations³⁰ and $N^*(E_F)=(1+\lambda)N(E_F)$, we estimate for the electron-phonon-coupling parameter $\lambda=0.62$. A reasonably sharp transition to superconductivity at T_{c1} can be clearly observed for $x=0.25$; the existence of a lower magnetic transition is indicated by the increase of $C(T)$ below about 3.5 K. For both compositions small tails of the magnetic contributions up to about 8 K ($x=0.25$) and 11 K ($x=0.45$) can

be observed. This could be due to a statistical distribution of the Gd atoms or to short-range fluctuations. The origin of the anomaly found in the $x=0.45$ data at about 6 K is not clear. If one assumes an impurity phase, or e.g., the correct tetragonal phase, however, with all R sites occupied by Gd, its volume is estimated to about 1%. We calculated the magnetic contribution ΔC to the specific heat by subtracting the nonmagnetic contribution using data from literature for the Y compound and Lu compound.^{34,35} For $x=0.45$ we find a jump in ΔC at the ordering temperature of $\Delta C/R_G=0.67$, corresponding well to $0.45 \times 1.5=0.68$, which is indicative of an effective $s=\frac{1}{2}$ system in molecular-field theory and R_G is the gas constant. From a linear extrapolation of the $\Delta C/R_G$ data to $T=0$ for $x=0.45$, we find a magnetic contribution to the entropy of $\Delta S/R_G=0.78$ corresponding to about 83% of $0.45 \ln(2J+1)$ with $J=\frac{7}{2}$ as theoretically expected.

IV. CONCLUSIONS

The behavior of $T_{c1}(x)$ of the $\text{Gd}_x\text{Y}_{1-x}\text{Rh}_4\text{B}_4$ system can be explained by AG theory for $x \leq 0.30$. The strength of the exchange interaction of the conduction electrons with the localized Gd moments is

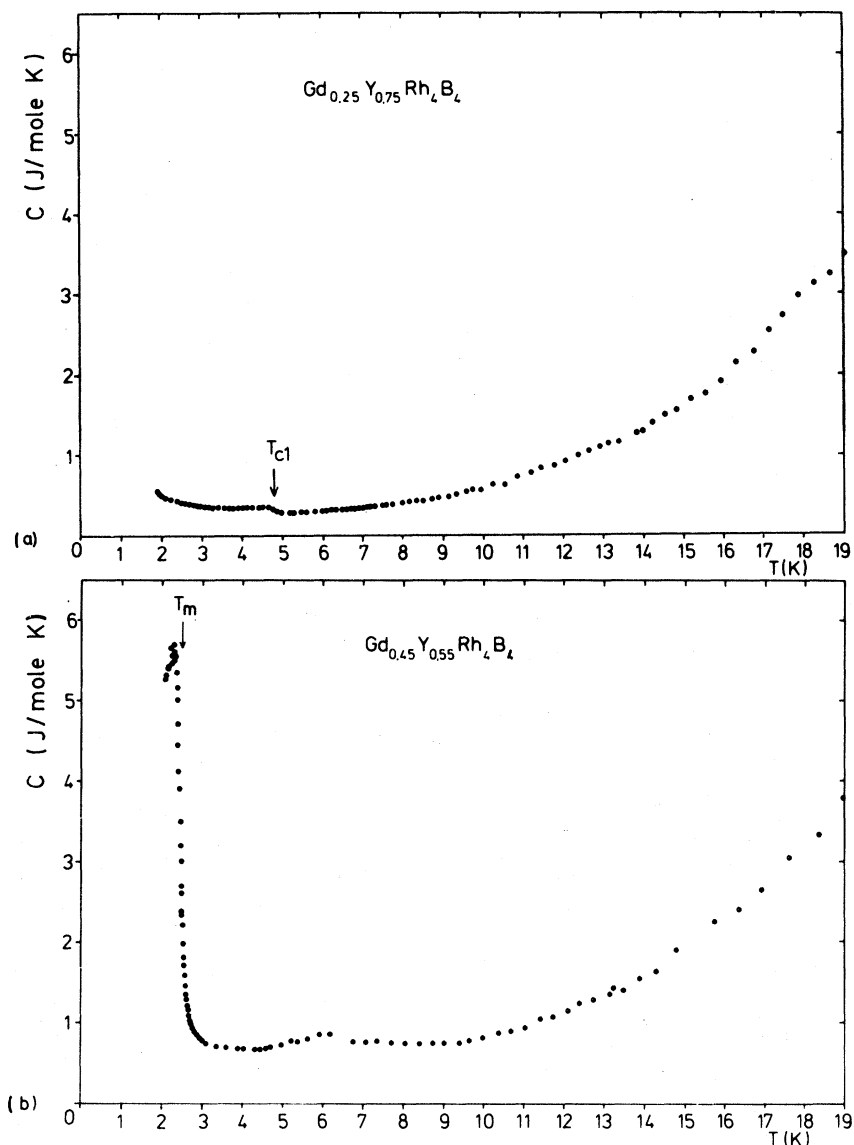


FIG. 14. Temperature dependence of the specific heat $C(T)$ for (a) $x=0.25$ and (b) $x=0.45$. The arrows indicate the normal to superconducting transition at T_{c1} and the magnetic transition at T_m . For further details, see text.

sufficient to mediate the indirect exchange interaction between the Gd ions which leads to ferromagnetic ordering for $x > 0.1$. The indirect nature of the Gd-Gd interaction follows also from an analysis of the ordering temperature with a theory introduced by Oguchi and Obokata³³ for diluted ferromagnets which shows that the Ising model is appropriate.

Magnetization measurements reveal extreme irreversible type-II behavior with large amounts of trapped flux at zero field. With decreasing temperature, the field intervals in which the samples with $x > 0.10$ change from the Meissner state to the

normal state decrease, indicating a transition towards type-II/1 or type-I superconductivity. Regarding M_{c2} , the magnetization at H_{c2} , our data clearly show that macroscopic electromagnetic effects are of far less importance in this system than in the $\text{Er}_{1-x}\text{Ho}_x\text{Rh}_4\text{B}_4$ system.

The temperature and concentration dependence of the lower critical fields H_{c1} as obtained from the magnetization measurements can be described by scaling behavior with T_{c1} and the shape of a non-magnetic superconductor down to temperature close above T_{c2} . Contrary to this, $H_{c2}(T)$ appears bell shaped for $x \geq 0.10$. The maximum of $H_{c2}(T)$ de-

creases exponentially with x . Surprisingly the temperature where this maximum occurs does not increase monotonically with x , but decreases with $x \geq 0.10$.

The normal-state susceptibility as determined by M_{c2}/H_{c2} or from Arrott plots follows Curie-Weiss laws with Curie temperatures increasing approximately linearly from $x=0.10$. From this we find within the Ising model an effective interaction strength of $3.8 \mu\text{eV}$ and a coordination number $z=12$ in agreement with the R sublattice. The Arrott plots also show the existence of spontaneous magnetization below the ordering temperature.

In high-field magnetization measurements only about 70% to 80% of the expected free-ion moment is obtained. Another indication for the tendency of the Gd moments to align anisotropically parallel to particular directions, presumably in the tetragonal basal plane, is given by the development of a small hysteresis in the low-field magnetization curves in fields exceeding H_{c2} —observed with samples with

$x \geq 0.25$ at temperatures $T_{c2} < T < T_{c1}$.

From the specific-heat measurements we calculate the dressed electronic density of states $N^*(E_F)=0.57$ states/(atom eV spin), which appears not to be dependent on x and to agree with data published for the nonmagnetic Lu and Y compounds. The details of the magnetic transition are found to scale with the Gd concentration and nearly the full entropy contribution is obtained as expected for $L=0$ ions. The reasonably sharp transitions revealed also in the specific-heat data, superconducting as well as magnetic, indicate good sample homogeneity.

ACKNOWLEDGMENTS

The authors acknowledge technical assistance by the Siemens Forschungslaboratorien in Erlangen and financial support by the Bundesministerium für Forschung and Technologie.

- ¹B. T. Matthias, E. Corenzwit, J. M. Vandenberg, and H. E. Barz, *Proc. Natl. Acad. Sci. U.S.A.* **74**, 1334 (1977).
- ²J. M. Vandenberg and B. T. Matthias, *Proc. Natl. Acad. Sci. U.S.A.* **74**, 1336 (1977).
- ³W. A. Fertig, D. C. Johnston, L. E. DeLong, R. W. McCallum, M. B. Maple, and B. T. Matthias, *Phys. Rev. Lett.* **38**, 987 (1977).
- ⁴See, e.g., *Proceedings of the International Conference on Ternary Superconductors*, edited by G. K. Shenoy, B. D. Dunlap, and F. Y. Fradin (Elsevier, New York, 1981).
- ⁵S. K. Sinha, G. W. Crabtree, D. G. Hinks, and H. Mook, *Phys. Rev. Lett.* **48**, 950 (1982).
- ⁶H. B. MacKay, L. D. Woolf, M. B. Maple, and D. C. Johnston, *Phys. Rev. Lett.* **42**, 918 (1979).
- ⁷H. R. Ott, W. A. Fertig, D. C. Johnston, M. B. Maple, and B. T. Matthias, *J. Low Temp. Phys.* **33**, 159 (1978).
- ⁸H. Adrian, K. Müller, and G. Saemann-Ischenko, *Phys. Rev. B* **22**, 4424 (1980).
- ⁹F. Behroozi, G. W. Crabtree, S. A. Campbell, M. Levy, D. Snider, D. C. Johnston, and B. T. Matthias, in *Proceedings of the International Conference on Ternary Superconductors*, Ref. 4, p. 155.
- ¹⁰D. C. Johnston, W. A. Fertig, M. B. Maple, and B. T. Matthias, *Solid State Commun.* **26**, 141 (1978).
- ¹¹M. B. Maple, H. C. Hamaker, D. C. Johnston, H. B. MacKay, and L. D. Woolf, *J. Less-Common Metals* **62**, 251 (1978).
- ¹²R. H. Wang, R. J. Laskowski, C. Y. Huang, J. L. Smith, and C. W. Chu, *J. Appl. Phys.* **49**, 1392 (1978).
- ¹³C. Y. Huang, S. E. Kohn, S. Maekawa, and J. L. Smith, *Solid State Commun.* **32**, 929 (1979).
- ¹⁴H. C. Ku, B. T. Matthias, and H. Barz, *Solid State Commun.* **32**, 937 (1979).
- ¹⁵K. Okuda, Y. Nakakura, and K. Kadowaki, *Solid State Commun.* **32**, 185 (1979).
- ¹⁶S. Maekawa, J. L. Smith, and C. Y. Huang, *Phys. Rev. B* **22**, 164 (1980).
- ¹⁷H. C. Ku, F. Acker, and B. T. Matthias, *Phys. Lett.* **76A**, 399 (1980).
- ¹⁸M. B. Maple, in *Proceedings of the International Conference on Ternary Superconductors*, Ref. 4, p. 131.
- ¹⁹F. Y. Fradin, P. K. Tse, and A. T. Aldred, in *Proceedings of the International Conference on Ternary Superconductors*, Ref. 4, p. 141.
- ²⁰H. Adrian, K. Müller, and G. Saemann-Ischenko, in *Proceedings of the International Conference on Ternary Superconductors*, Ref. 4, p. 175.
- ²¹R. C. Dynes, J. M. Rowell, and P. H. Schmidt, in *Proceedings of the International Conference on Ternary Superconductors*, Ref. 4, p. 169.
- ²²H. E. Mook, M. B. Maple, Z. Fisk, D. C. Johnston, and L. D. Woolf, in *Proceedings of the International Conference on Ternary Superconductors*, Ref. 4, p. 179.
- ²³L. D. Woolf and M. B. Maple, in *Proceedings of the International Conference on Ternary Superconductors*, Ref. 4, p. 181.
- ²⁴C. B. Vining and R. N. Shelton, in *Proceedings of the International Conference on Ternary Superconductors*, Ref. 4, p. 189.
- ²⁵H. B. MacKay, L. D. Woolf, M. B. Maple, and D. C. Johnston, *J. Low Temp. Phys.* **41**, 639 (1980).
- ²⁶M. Tachiki, H. Matsumoto, and H. Umezawa, *Phys.*

- Rev. B 20, 1915 (1979).
- ²⁷M. Tachiki, in *Proceedings of the International Conference on Ternary Superconductors*, Ref. 4, p. 267.
- ²⁸D. E. Moncton, G. Shirane, W. Thomlinson, Phys. Rev. Lett. 45, 2060 (1980).
- ²⁹A. A. Abrikosov and L. P. Gorkov, Zh. Eksp. Teor. Fiz. 39, 1781 (1960) [Sov. Phys.—JETP 12, 1243 (1961)]; Zh. Eksp. Teor. Fiz. 43, 2230 (1962) [Sov. Phys.—JETP 16, 1575 (1963)].
- ³⁰T. Jarlborg, A. J. Freeman, and T. J. Watson-Yang, Phys. Rev. Lett. 39, 1032 (1977).
- ³¹H. R. Ott, H. Rudigier, H. C. Hamaker, and M. B. Maple, in *Proceedings of the International Conference on Ternary Superconductors*, Ref. 4, p. 159.
- ³²Reanalyzing our magnetization data on the $\text{Er}_{1-x}\text{Ho}_x\text{Rh}_4\text{B}_4$ we find indications of this effect at low temperatures. However, at that time we did not measure complete hysteresis loops and failed to realize its significance. We attributed it to an insufficient stability of the integrating system and to relaxation phenomena (decay of aligned magnetic moments) which have been observed to become significant in decreasing field for $\dot{H} > 4 \times 10^3 \text{ A m}^{-1} \text{ s}^{-1}$ at low temperatures.
- ³³T. Oguchi and T. Obokata, J. Phys. Soc. Jpn. 27, 1111 (1969).
- ³⁴L. D. Woolf, D. C. Johnston, H. B. MacKay, R. W. McCallum, and M. B. Maple, J. Low Temp. Phys. 35, 651 (1979).
- ³⁵K. Kumagai, Y. Inoue, and K. Asayama, J. Phys. Soc. Jpn. 47, 1363 (1979).